COBEM2003 - 1818 Copyright © 2003 by ABCM

DESIGN OF LAYERED PIEZOELECTRIC PLATE AND SHELL STRUCTURES FOR MINIMUM COMPLIANCE USING TOPOLOGY OPTIMIZATION

Martin Kögl
Department of Structures and Foundation Engineering
University of São Paulo
Av. Prof. Almeida Prado Trav. 2, 83
05508-900 São Paulo, SP, Brazil
e-mail: m_koegl@yahoo.com

Emílio C. N. Silva
Department of Mechatronics and Mechanical Systems Engineering
University of São Paulo
Av. Prof. Mello Moraes, 2231
05508-900 São Paulo, SP, Brazil
e-mail: ecnsilva@usp.br

Miguel L. Bucalem
Department of Structures and Foundation Engineering
University of São Paulo
Av. Prof. Almeida Prado Trav. 2, 83
05508-900 São Paulo, SP, Brazil
e-mail: mlbucale@usp.br

Abstract: *The stiffness of multi-layer plate and shell structures can be increased by employing piezoelectric layers and making use of the piezoelectric coupling effect. It is well-known that the actuation performance to increase stiffness depends on the distribution of material in the piezoelectric layers. Motivated by this idea, the concept of topology optimization is applied in this work to determine the optimal distribution of piezoelectric material in a multi-layer plate or shell structure to provide the minimum compliance when actuated. This should be achieved with a limited amount of piezoelectric material, e.g., to reduce the weight of the structure. Topology optimization is a powerful structural optimization method that combines the Finite Element Method (FEM) with an optimization algorithm to find the optimal material distribution inside a given domain. The topology optimization applied in the present work is based on the so-called SIMP (Solid Isotropic Material with Penalization) model, for which an extension to piezoelectric materials is proposed that allows the algorithm to choose the optimum polarization of the piezoelectric material in each element. For the modeling of the piezoelectric layers, newly developed piezoelectric plate and shell finite elements are employed, which are free of locking and allow an accurate modeling of thin piezoelectric actuators of arbitrary geometry. The potential of the proposed method is demonstrated by a numerical example, where an excellent performance of the enhanced piezoelectric SIMP model is observed, confirming the importance of including the polarization as an additional design variable in the optimization process.*

Keywords: *piezoelectricity, plate analysis, topology optimization, SIMP model, finite element method*

1. Introduction

Layered piezoelectric plates and shells, such as those encountered in smart structures, are composite structures made of piezoelectric and elastic materials. Usually, the piezoelectric layers are attached as sensors and/or actuators to the top and bottom surfaces of an elastic base layer, commonly an aluminium or steel structure. This allows a real-time sensing and actuation of the structural deformation so that, by employing a suitable control circuit, the deformation can be controlled. Possible applications of smart structures include the shape control of airplane wings (Chattopadhyay et al., 1999), car bodies, reflector antennas (Agrawal and Treanor, 1999), deformable mirrors, micromotors (Brei and Moskalik, 1997), etc. For the actuation, usually piezoceramics such as PZT are employed, while piezoelectric polymers like PVDF are used as sensors.

Owing to the large number of applications, the computational modeling of (layered) piezoelectric plates and shells has been extensively studied in the past few years, mainly using the Finite Element Method (see, e.g., Tzou and Tseng, 1990; Saravanos, 1997a,b; Kögl and Bucalem, 2002,2003). The distribution of piezoelectric material over the plate or shell surface can be used to influence its structural characteristics, e.g., to increase the stiffness, generate a desired displacement for a given applied voltage, or to improve the vibration control of the structure. Thus, a very important question to be addressed in the design of smart structures concerns the optimal distribution of piezoelectric material over the plate or shell. Many authors have studied this problem in the past few years, usually by trying to find the optimal placement of small pieces of piezoceramics on the plate or shell structure by using optimization algorithms (Chattopadhyay et al., 1999; Mukherjee and Joshi, 2002). Recently, some authors have begun to apply sizing optimization techniques to find an optimal distribution of

the piezoelectric layer over plate or shell structures, with very promising results (Mukherjee and Joshi, 2002). However, some of the applied optimization techniques are empiric and no systematic approach was developed.

In a number of smart structures applications, the piezoelectric coupling effect is employed to increase the structural stiffness. This can be achieved by using the piezoelectric layers as actuators, since the deformation induced by the applied voltage or electric charge influences the structural stiffness. The objective of optimization is then to obtain a maximum stiffness for a limited amount of piezoelectric material, e.g., to reduce the weight of the structure. Motivated by this idea, the present work applies the concept of topology optimization to find the optimal distribution of material in a piezoelectric layer in a composite plate or shell structure to provide the minimum compliance when actuated. The presented approach is quite general and can be employed not only for the design of layered piezoelectric plates and shells in smart structures, but also for a number of different applications.

Topology optimization is a powerful structural optimization method that combines a numerical solution method, usually the Finite Element Method, with an optimization algorithm to find an optimal material distribution inside a given domain (Bendsøe and Sigmund, 2003). The topology optimization applied in the present work is based on the so-called SIMP (Solid Isotropic Material with Penalization) model, which is extended to piezoelectric materials in a way to allow a sign change of the electric polarization in each element. Two design variables are employed for each element: the amount of piezoelectric material ("density") and the polarization of the material. In the Finite Element calculations, newly developed piezoelectric plate and shell elements are employed, which are free of locking, reliable, and allow an accurate modeling of thin piezoelectric sensors and actuators of arbitrary geometry. For the optimization, sequential linear programming (SLP) is used. The potential of the proposed method is demonstrated by a numerical example, where an excellent performance of the enhanced piezoelectric SIMP model is observed.

The paper is organized as follows. In Section 2, the Finite Element modeling of piezoelectric plates and shells is briefly reviewed. In Section 3, the concept of topology optimization and the formulation of the optimization problem are described. Section 4 discusses the numerical implementation of the optimization problem. In Section 5, results are presented to illustrate the proposed method and finally, in Section 6, some conclusions are given.

2. Finite Element Modeling of Piezoelectric Plates and Shells

At each iteration of the topology optimization procedure, a structural analysis has to be performed. This is usually done with the Finite Element Method (FEM) (Bathe, 1996). It is very important that the finite elements used in the analysis be reliable and accurate, so that the optimization procedure can yield good results. In the analysis of piezoelectric plates and shells, this means that the elements must not present locking, and that they should be able to model accurately the piezoelectric coupling. Recently, new piezoelectric plate and shell elements that fulfil these requirements have been presented by two of the authors (Kögl, 2002; Kögl and Bucalem, 2003), and these elements were used in the analyses described in this paper. Some features of the elements that are relevant in the context of this article will be briefly revised in the following.

The elements are based on the Reissner-Mindlin kinematic assumptions and their generalization to shells. For the electric field, a quadratic variation of the electric potential over the thickness is assumed by introducing mid-surface electric degrees of freedom (Kögl and Bucalem, 2003), so that the elements can model accurately the electric potential induced in bending deformations. To eliminate locking, assumed natural strain fields in the form of the MITC approach are used (Bucalem and Bathe, 1997). With these assumptions, one obtains for the elastic strains $\boldsymbol{\varepsilon}$ and the electric field $\boldsymbol{E}$ at the nodes (for a detailed description, see (Kögl, 2002))

$$\boldsymbol{\varepsilon} = \boldsymbol{B}_\varepsilon \, \boldsymbol{u} \qquad \text{and} \qquad \boldsymbol{E} = -\boldsymbol{B}_E \, \boldsymbol{\varphi} \, , \tag{1}$$

where $\boldsymbol{u}$ contains the elastic degrees of freedom (displacements and section rotations), and $\boldsymbol{\varphi}$ contains the electric potential degrees of freedom. The transformation matrices $\boldsymbol{B}_\varepsilon$ and $\boldsymbol{B}_E$ depend only on the geometry and not on the material properties, which is important in the derivation of the sensitivities described in Section 3.2. With the piezoelectric constitutive equations (Gaul et al., 2003), this yields the element stiffness matrices

$$\boldsymbol{K}_{uu}^{(e)} = \int_{\Omega^{(e)}} \boldsymbol{B}_\varepsilon^{\mathrm{T}} \, \boldsymbol{C} \, \boldsymbol{B}_\varepsilon \; \mathrm{d}\Omega \, , \qquad \boldsymbol{K}_{u\varphi}^{(e)} = \int_{\Omega^{(e)}} \boldsymbol{B}_\varepsilon^{\mathrm{T}} \, \boldsymbol{e} \, \boldsymbol{B}_E \; \mathrm{d}\Omega \, , \qquad \boldsymbol{K}_{\varphi\varphi}^{(e)} = -\int_{\Omega^{(e)}} \boldsymbol{B}_E^{\mathrm{T}} \, \boldsymbol{\epsilon} \, \boldsymbol{B}_E \; \mathrm{d}\Omega \, , \tag{2}$$

where $\boldsymbol{C}$, $\boldsymbol{e}$, and $\boldsymbol{\epsilon}$ are the elasticity matrix, piezoelectric matrix, and permittivity matrix, respectively; the superscript (e) denotes the element. The final discretized FEM system of equations can then be written as

$$\begin{bmatrix} \boldsymbol{K}_{uu} & \boldsymbol{K}_{u\varphi} \\ \boldsymbol{K}_{u\varphi}^{\mathrm{T}} & \boldsymbol{K}_{\varphi\varphi} \end{bmatrix} \begin{bmatrix} \boldsymbol{u} \\ \boldsymbol{\varphi} \end{bmatrix} = \begin{bmatrix} \boldsymbol{F} \\ \boldsymbol{Q} \end{bmatrix} \qquad \text{or} \qquad \boldsymbol{K}\boldsymbol{U} = \boldsymbol{\mathcal{Q}} \, , \tag{3}$$

with $(\cdot)^{\mathrm{T}}$ denoting the transpose of the matrix. Note that the charge vector $\boldsymbol{Q}$ has non-zero elements only at the electrodes since the electric charges are zero inside the piezoelectric material.

3. Formulation of Topology Optimization Problem

Topology optimization is based on two main concepts (Bendsøe and Kikuchi, 1988; Bendsøe and Sigmund, 2003): the extended design domain and a suitable material model. The extended design domain is a large fixed domain that must contain the whole structure to be determined by the optimization procedure. The objective of topology optimization is to determine the holes and connectivities of the structure by adding and removing material in this domain. Thus, the topology optimization problem is defined as a problem of finding the optimal distribution of material in the extended domain. Since the extended domain is fixed, the Finite Element model domain is not changed during the optimization process, which simplifies the calculation of derivatives of any function defined over the extended domain. In the current problem the design domain has the size of the elastic base layer, since piezoelectric material can only be added on top or bottom of this base layer.

3.1. An Extended SIMP Model for Piezoelectricity

If the amount of material in each element could assume only values equal to either one or zero, the material distribution function would be discrete and very discontinuous. This would present difficulties in the numerical treatment of the problem. To overcome this, the concept of a continuous material model is introduced. Essentially, the material model approximates the material distribution by defining a function of a continuous parameter that determines a mixture of two materials throughout the domain. By allowing the appearance of intermediate (or composite) materials – rather than only void or full material – in the final solution, this provides enough relaxation for the design problem.

The material model employed in the present work is based on the so-called SIMP (Solid Isotropic Material with Penalization) model. This model was initially defined for elastic materials (Bendsøe, 1989) and was recently extended to piezoelectric materials (Silva and Kikuchi, 1999). However, it did not allow a sign change of the piezoelectric polarization during optimization. In the design of piezoelectric plates or shells, this is very important since the actuators must be able to both expand and contract. Although in practice this is achieved by applying either positive or negative charges to the electrodes, the numerical implementation is considerably simplified by treating this as a change of sign of the polarization. Otherwise, the design domain would not remain fixed, but separate electrodes with different charges would appear and disappear during the optimization, which would introduce an enormous difficulty into the analysis.

Therefore, in this paper, a more comprehensive SIMP material model for piezoelectric materials is proposed which allows to change the sign of the piezoelectric matrix $\boldsymbol{e}$ – and as a result the polarity of the piezoelectric material – by introducing a new design variable ρ_2:

$$\boldsymbol{C} = \rho_1^{p_c}\,\boldsymbol{C}_0\ , \tag{4}$$

$$\boldsymbol{e} = \rho_1^{p_e}\,(2\rho_2-1)^{p_i}\,\boldsymbol{e}_0\ , \tag{5}$$

$$\boldsymbol{\epsilon} = \rho_1^{p_\epsilon}\,\boldsymbol{\epsilon}_0\ . \tag{6}$$

In Eqs (4)–(6), ρ_1 is a pseudo-density describing the amount of material in each finite element, and ρ_2 describes the polarization. Both ρ_1 and ρ_2 can assume values between 0 and 1. The matrices $\boldsymbol{C}_0$, $\boldsymbol{e}_0$, and $\boldsymbol{\epsilon}_0$ contain the components of the elasticity, piezoelectricity, and permittivity tensors of the 'real' material. Even though intermediate (composite) materials are allowed during the optimization, the final topology should contain only values of ρ_1 and ρ_2 equal to (or very close to) 0 or 1. To achieve this, following the idea of the original SIMP model, penalization factors p_c, p_e, and p_ϵ are employed to penalize intermediate densities. For an elastic material, the optimum value for p_c was found to be equal to 3 (Bendsøe and Sigmund, 2003). In the present paper, the same value will be used for all exponents of ρ_1, i.e, $p_c = p_e = p_\epsilon = 3$; in addition, $p_i = 1$. The effect of using other values for the penalization factors is not addressed here but is currently the subject of investigation.

Regarding the expression (6) for the permittivity $\boldsymbol{\epsilon}$, one may argue that from a physical point of view the minimum possible value is not zero but the vacuum permittivity ϵ_{vac}, thus a correct expression would be:

$$\boldsymbol{\epsilon} = \rho_1^{p_\epsilon}\,\boldsymbol{\epsilon}_0 + (1-\rho_1^{p_c})\,\boldsymbol{I}\epsilon_{\text{vac}}\ , \tag{7}$$

where $\boldsymbol{I}$ is the 3×3 identity matrix. However, using the simplification (6) does not present any numerical difficulties, and since for $\rho_1 \to 0$ the material vanishes anyway, expression (6) is a reasonable approximation and will be employed to simplify the implementation.

3.2. Formulation of Design Problem

The problem of minimum compliance design for elastic plate and shell structures has been extensively studied in the literature (see for example (Suzuki and Kikuchi, 1991; Díaz et al., 1995; Kumar and Gossard, 1996)). However, to the authors' knowledge, no investigations have been carried out so far dealing with the minimum compliance problem for thin piezoelectric plate or shell structures.

It is well-known that the stiffness of a piezoelectric plate can be changed by applying an electric charge, an effect that is commonly employed in the control of piezoelectric plates. Hence, the minimum compliance design problem for piezoelectric structures should not be considered by defining as objective function the minimum (elastic) compliance function $\boldsymbol{u}^{\mathrm{T}}\boldsymbol{F}$ alone, since a large electrical energy may be necessary to achieve this minimum compliance. Instead, the objective function for the minimum compliance design problem for piezoelectric structures should also take into account the electrical energy.

Consider a piezoelectric plate domain as shown in Fig. 1, which is subjected to an input electric charge Q in an electrode (region Γ_q) and mechanical tractions t_i in region Γ_t. Then the optimization problem for a

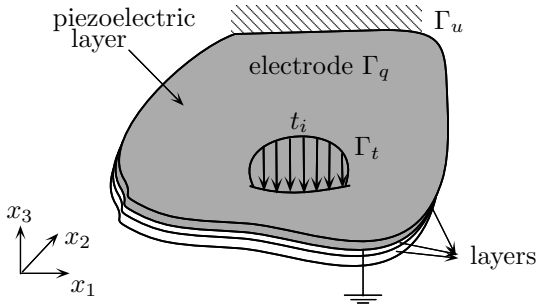

Figure 1: Layered piezoelectric plates subjected to mechanical loads t_i and electric charges Q

piezoelectric layered structure is obtained by minimizing the so-called mean compliance

$$L(u_i, \varphi) := \int_{\Gamma_t} t_i u_i \, \mathrm{d}\Gamma - \int_{\Gamma_q} q\,\varphi \, \mathrm{d}\Gamma \,, \tag{8}$$

where $q = -D_i n_i$ is the electric charge density. In the case of piezoelectric plate and shell structures, the region Γ_q corresponds to the electrodes attached to the piezoelectric layers, as shown in Fig. 1. Since the electrodes are equipotential surfaces, it follows that $\int q\,\varphi \, \mathrm{d}\Gamma = Q\,\varphi$, which is the electrical work used to increase the plate stiffness. By minimizing the mean compliance function L, the structural compliance is thus minimized with the minimum amount of electrical energy. Observe that the definition (8) is similar to the mean compliance function defined in (Silva et al., 2000).

Expressing now the mean compliance in terms of the discretized equilibrium equation (3), one obtains

$$L(\boldsymbol{u}, \boldsymbol{\varphi}) \;\; = \;\; \boldsymbol{u}^{\mathrm{T}}\boldsymbol{F} + \boldsymbol{\varphi}^{\mathrm{T}}\boldsymbol{Q} = \begin{bmatrix} \boldsymbol{u} \\ \boldsymbol{\varphi} \end{bmatrix}^{\mathrm{T}} \begin{bmatrix} \boldsymbol{K}_{uu} & \boldsymbol{K}_{u\varphi} \\ \boldsymbol{K}_{u\varphi}^{\mathrm{T}} & \boldsymbol{K}_{\varphi\varphi} \end{bmatrix} \begin{bmatrix} \boldsymbol{u} \\ \boldsymbol{\varphi} \end{bmatrix} . \tag{9}$$

Note that if either no electric charges are applied to the electrodes ($\boldsymbol{Q} = \boldsymbol{0}$) or if the electrodes are short-circuited ($\boldsymbol{\varphi} = \boldsymbol{0}$), then the electrical work is zero, and the problem becomes equal to the traditional minimum compliance design problem. It should be mentioned here that the piezoelectric stiffness matrix $\boldsymbol{K}$ as given in Eq. (3) is indefinite, which suggests that the minimum mean compliance design problem for piezoelectric structures may be non-convex, in contrast to the traditional minimum compliance design problem. Essentially, Eq. (9) describes a multi-objective function given by the linear combination of the mechanical and electrical compliances, where the weights are the applied force and electric charge. Thus, depending on the values of the applied forces and electric charges, the optimization algorithm will focus more on the electrical than on the mechanical compliance, or vice versa.

Now, to minimize the mean compliance of a piezoelectric structure, the following optimization problem must be solved:

$$\begin{array}{ll} \text{Minimize:} & L(\boldsymbol{u}, \boldsymbol{\varphi}) \\ \rho_1, \rho_2 \text{ subject to:} & \boldsymbol{K}\boldsymbol{U} = \boldsymbol{\Omega} \text{ (FEM equilibrium equations)} \\ & 0 < \rho_{\min} \leq \rho_1 \leq 1 \\ & 0 \leq \rho_2 \leq 1 \\ & \Theta_0 \leq \Theta(\rho_1) = \frac{1}{S}\int \rho_1 \, \mathrm{d}S \leq \Theta_1 \,, \end{array}$$

where S is the volume of the design domain, Θ is the volume fraction, and $\{\Theta_0, \Theta_1\} \in [0, 1]$ are the lower and upper bounds on the amount of material to be used in the piezoelectric layer. The other constraints are the equilibrium equations (3) and box constraints for the design variables ρ_1 and ρ_2 in each element. The lower bound $\rho_{\min} = 0.001$ specified for ρ_1 is necessary to avoid numerical problems that would result if the stiffness matrix became singular. Since regions with $\rho_1 = 0.001$ have virtually no structural significance, for all practical purposes they can be considered regions without piezoelectric material in the final design.

Notice that the electrical excitation is provided by the electric charges Q applied to the electrodes, which are isopotential surfaces. Hence, by reducing the amount of piezoelectric material in certain regions of the

domain, the electric charge density $q = \mathrm{d}Q/\,\mathrm{d}S$ is increased. This yields also an increase in the electric field in regions where piezoelectric material is present. However, the electric field must at no point exceed the maximum admissible field strength that the piezoelectric material can support without being damaged. To ensure this, the electric field can be indirectly controlled by adjusting the lower volume constraint Θ_0 in the optimization problem.

3.3. Calculation of Sensitivities

To solve the optimization problem with the SLP algorithm, it is necessary to calculate the sensitivities (or gradients) of the objective function L and constraints with respect to ρ_1 and ρ_2. The gradient of the volume constraint is straightforward. The sensitivity of the objective function $L = \boldsymbol{U}^{\mathrm{T}}\boldsymbol{\Omega}$ with respect to ρ (where ρ can be either ρ_1 or ρ_2) is obtained by considering that $\partial\boldsymbol{\Omega}/\partial\rho = \boldsymbol{0}$, thus

$$\frac{\partial L}{\partial \rho} = \frac{\partial \boldsymbol{U}^{\mathrm{T}}}{\partial \rho}\boldsymbol{\Omega} \,. \tag{10}$$

Equally, it follows for the derivative of the equilibrium equation $\boldsymbol{K}\boldsymbol{U} = \boldsymbol{\Omega}$:

$$\frac{\partial \boldsymbol{K}}{\partial \rho}\boldsymbol{U} + \boldsymbol{K}\frac{\partial \boldsymbol{U}}{\partial \rho} = \boldsymbol{0} \,. \tag{11}$$

Substituting this into Eq. (10) yields

$$\frac{\partial L}{\partial \rho} = \frac{\partial \boldsymbol{U}^{\mathrm{T}}}{\partial \rho}\boldsymbol{K}\boldsymbol{U} = -\boldsymbol{U}^{\mathrm{T}}\frac{\partial \boldsymbol{K}}{\partial \rho}\boldsymbol{U} \,. \tag{12}$$

With the material model proposed in Eqs (4)–(6), the sensitivities of the stiffness matrices with respect to the design variables ρ_1 and ρ_2 are given by

$$\begin{aligned}
&\frac{\partial \boldsymbol{K}_{uu}}{\partial \rho_1} = p_c\frac{\boldsymbol{K}_{uu}}{\rho_1} \,, && \frac{\partial \boldsymbol{K}_{u\varphi}}{\partial \rho_1} = p_e\frac{\boldsymbol{K}_{u\varphi}}{\rho_1} \,, && \frac{\partial \boldsymbol{K}_{\varphi\varphi}}{\partial \rho_1} = p_\epsilon\frac{\boldsymbol{K}_{\varphi\varphi}}{\rho_1} \,, \\
&\frac{\partial \boldsymbol{K}_{uu}}{\partial \rho_2} = \boldsymbol{0} \,, && \frac{\partial \boldsymbol{K}_{u\varphi}}{\partial \rho_2} = 2p_i\,\frac{\boldsymbol{K}_{u\varphi}}{(2\rho_2 - 1)} \,, && \frac{\partial \boldsymbol{K}_{\varphi\varphi}}{\partial \rho_2} = \boldsymbol{0} \,.
\end{aligned} \tag{13}$$

This yields

$$\frac{\partial \boldsymbol{K}}{\partial \rho_1} = \frac{1}{\rho_1}\begin{bmatrix} p_c\,\boldsymbol{K}_{uu} & p_e\,\boldsymbol{K}_{u\varphi} \\ p_e\,\boldsymbol{K}_{u\varphi}^{\mathrm{T}} & p_\epsilon\,\boldsymbol{K}_{\varphi\varphi} \end{bmatrix} \qquad \text{and} \qquad \frac{\partial \boldsymbol{K}}{\partial \rho_2} = \frac{2p_i}{2\rho_2 - 1}\begin{bmatrix} \boldsymbol{0} & \boldsymbol{K}_{u\varphi} \\ \boldsymbol{K}_{u\varphi}^{\mathrm{T}} & \boldsymbol{0} \end{bmatrix} \,, \tag{14}$$

and the sensitivities of the objective function with respect to the design variables are obtained by substitution into Eq. (12).

4. Numerical Implementation

A flow chart of the optimization algorithm is shown in Fig. 2. The algorithm was implemented in the first author's Finite Element program CoFAS, employing the newly developed piezoelectric plate and shell elements described in Section 2. The structures can consist of an arbitrary number of layers, which are assumed to be perfectly bonded. The design domain for the topology optimization contains only the piezoelectric layer(s). The design variables are the pseudo-densities ρ_1 and ρ_2, which can assume different values for each finite element. The Finite Element equilibrium equation (3) is solved at each iteration step using a direct skyline solver.

In this study, owing to the large number of design variables, Sequential Linear Programming (SLP) is employed to solve the optimization problem (Hanson and Hiebert, 1981; Vanderplaatz, 1984). The problem is linearized by developing the objective function and constraints into Taylor series at each iteration up to the linear term. This requires the sensitivities (gradients) with respect to ρ_1 and ρ_2 as derived in Section 3.3. Suitable move limits are introduced to assure that the design variables do not change by more than 5–15% between consecutive iterations. A new set of design variables ρ_1 and ρ_2 is obtained after each iteration, which continues until convergence is achieved for the objective function. Uniform values for ρ_1 and ρ_2 are used as an initial guess.

When the optimization process has converged, the result is an optimum distribution of the densities ρ_1 and ρ_2 over the mesh. This distribution may contain intermediate values for the densities ("gray scale") representing an intermediate material, but the results need to be interpreted as a distribution of two phases ("black" and "white"), which are easier to manufacture in practice. In this work, no special filtering is employed, using only an ordinary threshold value to represent the optimum topology as a black and white image.

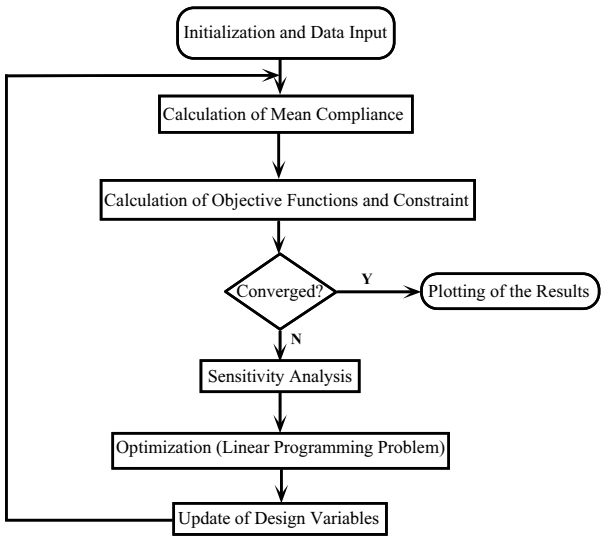

Figure 2: Flow chart of optimization procedure

5. Results

An example is presented to illustrate the minimum mean compliance design for a piezoelectric plate structure using the proposed method. A quadratic plate with sidelength $L = 300$ mm is clamped at two sides Γ_1 and Γ_2 (u_y is not constrained at Γ_2) and is subjected to a unit point force at A(240 mm,210mm), as shown in Fig. 3. The plate is made of aluminium, with Young's modulus $E = 71$ GPa and Poisson's ratio $\nu = 0.334$, and has a

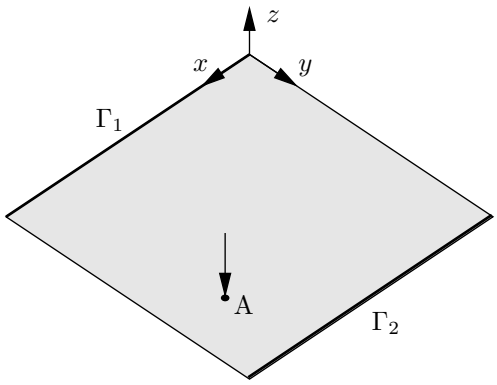

Figure 3: Quadratic plate clamped at sides Γ_1 and Γ_2, and subjected to a unit point force at A

thickness of $a_0 = 1$ mm. On top of the aluminium layer, a piezoelectric layer made of the piezoceramic PZT is attached, with a thickness of $a_1 = 0.2$ mm. In matrix notation, the material properties of PZT are given by

$$\boldsymbol{C} = \begin{bmatrix} 107.6 & 63.1 & 63.9 & 0 & 0 & 0 \\ 63.1 & 107.6 & 63.9 & 0 & 0 & 0 \\ 63.9 & 63.9 & 100.4 & 0 & 0 & 0 \\ 0 & 0 & 0 & 19.6 & 0 & 0 \\ 0 & 0 & 0 & 0 & 19.6 & 0 \\ 0 & 0 & 0 & 0 & 0 & 22.2 \end{bmatrix} \text{GPa} , \tag{15}$$

$$\boldsymbol{e} = \begin{bmatrix} 0 & 0 & 0 & 0 & 12.0 & 0 \\ 0 & 0 & 0 & 12.0 & 0 & 0 \\ -9.6 & -9.6 & 15.1 & 0 & 0 & 0 \end{bmatrix} \text{N/Vm} , \tag{16}$$

$$\boldsymbol{\epsilon}^{\text{rel}} = \begin{bmatrix} 1936 & 0 & 0 \\ 0 & 1936 & 0 \\ 0 & 0 & 2109 \end{bmatrix} , \tag{17}$$

where $\boldsymbol{\epsilon}^{\text{rel}}$ are the relative permittivities.

In the following, the piezoelectric layer is chosen to be the design domain, and a constant charge Q is applied to the electrode attached to the piezoelectric layer. The optimization problem now consists in finding

the optimum distribution of piezoelectric material in this layer and choosing a suitable polarization for each element, so as to minimize the mean compliance. A mesh of 30×30 piezoelectric plate elements is used for the Finite Element analysis. The volume constraint is chosen as $\Theta_0 = \Theta_1 = 0.3$, i.e., the piezoelectric shall be distributed over 30 % of the plate area. Since the volume is prescribed and does not change during the iterations, the optimization procedure needs to start with an initial volume constraint of $\Theta = 0.3$, to guarantee that the optimization problem starts in the feasible domain (all constraints satisfied).

5.1. Stability Considerations

The optimization procedure is carried out with different electric charges Q, since the optimum charge is not known in advance. The resulting optimum topologies after 20 iterations are shown in Fig. 4, where the '+' and '-' sign indicate positive and negative polarization, respectively. The image labelled 'elastic analysis' shows the solution of the elastic minimum compliance problem, for which the piezoelectric matrix was set to zero ($\boldsymbol{d} = \boldsymbol{0}$).

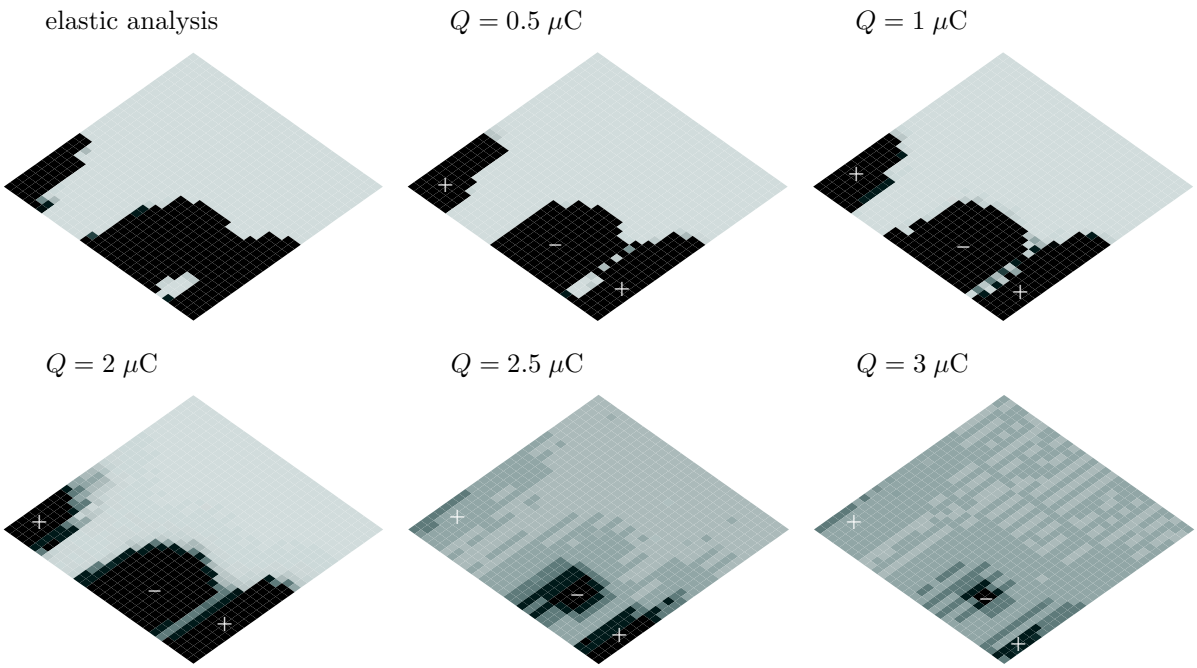

Figure 4: Optimal topologies (ρ_1) for different applied charges Q; '+' indicates positive polarization, '-' indicates negative polarization of the respective electrode

Tab. 1 gives the ratio between the electric energy $W^{\varphi} = Q\,\varphi$ and the elastic energy $W^{u} = F^{\mathrm{A}}\,u_z^{\mathrm{A}}$. Observe that for small charges Q the topologies do not differ very much, but the picture changes rapidly when the charge reaches a critical value. Between $Q = 2.0\ \mu$C and $Q = 2.5\ \mu$C, the topologies start to become blurred and the displacement u_z^{A} (which has the same absolute value as W^{u} since F^{A} is a unit force) increases instead of decreasing. Regarding the ratio between the electric and elastic energies, one observes that for small Q the ratio increases only slowly, while for $Q > 2\ \mu$C, a drastic increase is observed, confirming the pattern instability observed in Fig. 4.

Table 1: Ratio between electric energy $W^{\varphi} = Q\,\varphi$ and elastic energy $W^{u} = F^{\mathrm{A}}\,u_z^{\mathrm{A}}$

Q [μC]	elast.	0.5	1.0	1.5	2.0	2.5	3.0
W^{φ} [μJ]	0.00	0.55	1.30	2.29	3.63	13.64	30.36
W^{u} [μJ]	56.93	53.57	53.15	52.88	52.69	63.32	74.62
W^{φ}/W^{u} [%]	0.00	1.02	2.45	4.33	6.89	21.54	40.68

This instability becomes also apparent when regarding the mean compliance during the iterations, as shown in Fig. 5. For $Q = 1.5\ \mu$C and $Q = 2\ \mu$C, the mean compliance converges smoothly, while for higher values of the charge Q the compliance oscillates, indicating that the optimization algorithm encounters difficulties in finding an optimum solution.

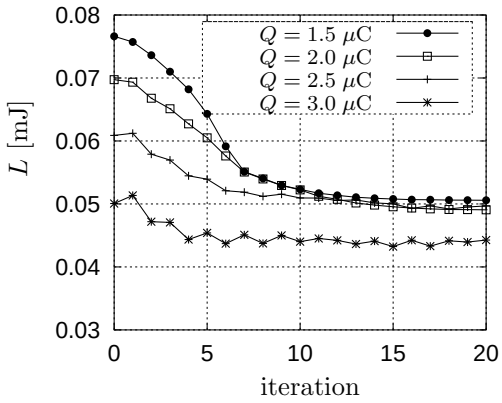

Figure 5: Mean compliance L for different charges Q

5.2. Inversion of Polarization

A very important aspect of the proposed optimization algorithm is the newly introduced inversion of polarization, described by the design variable ρ_2. As shown in Fig. 6 (left), three regions of opposite polarization ρ_2 can be distinguished: the bright region indicates negative polarization, while the dark regions indicate positive polarization. This leads to three clearly distinguishable electrodes in the final design, of which the middle one has negative polarization.

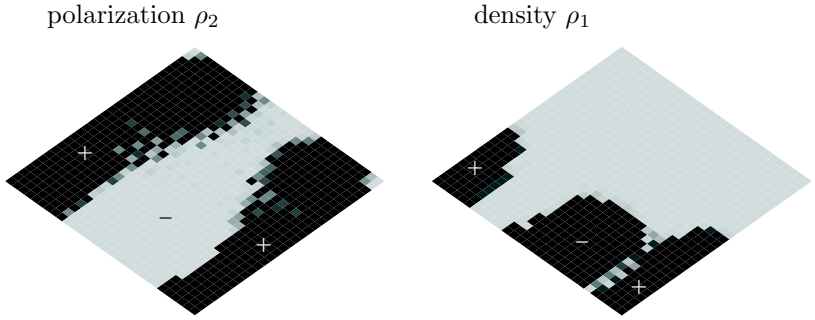

Figure 6: Optimum topology for $Q = 1$ μC: the choice of optimum polarization by the algorithm leads to three separate electrodes, of which the middle one has negative polarization

In Fig. 7, three different topologies are shown for $Q = 1$ μC. The first topology is obtained with the algorithm choosing the optimum polarization ($0 \leq \rho_2 \leq 1$) for each element, while the other topologies are obtained with a constant, fixed polarization throughout the piezoelectric layer, using a positive ($\rho_2 = 1$) and a negative ($\rho_2 = 0$) polarization.

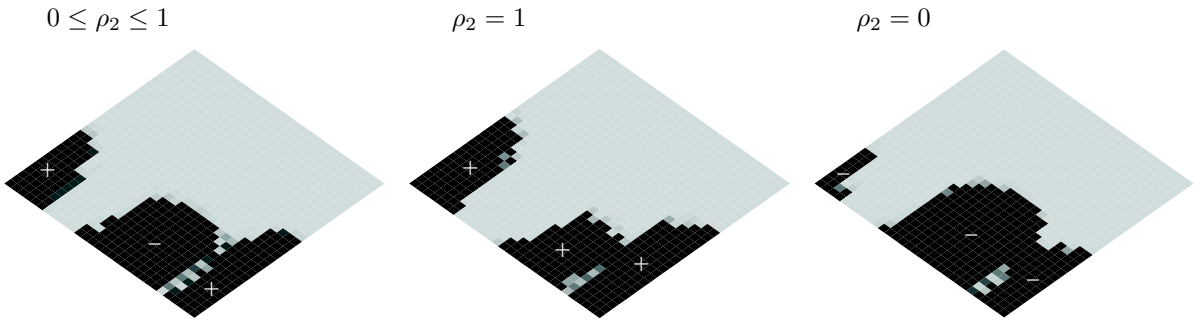

Figure 7: Optimum topologies (ρ_1) for $Q = 1$ μC: polarization ρ_2 chosen by the algorithm (left) or held constant (center, right)

Regarding the displacement at point A, given in Tab. 2, one observes that the lowest value is achieved when the algorithm optimizes the polarization. This is to be expected, since an optimal stiffness is obtained when some of the piezoelectric regions contract while others expand, which can only be achieved with opposite

Table 2: Displacement u_z at point A for $Q = 1$ μC and different constraints for the polarization ρ_2

polarization	u_z [μm]
$0 \leq \rho_2 \leq 1$	53.15
$\rho_2 = 1$	57.61
$\rho_2 = 0$	57.00

polarizations or applied charges. The results therefore confirm the excellent performance of the proposed new SIMP model for piezoelectrics including polarization, and the capacity of the algorithm to choose an optimum polarization.

Observe also that in Fig. 4, the topologies obtained with the piezoelectric material are very similar to the topology obtained solving the elastic minimum compliance problem (upper left image in Fig. 4). In this case, the distribution of material is carried out in such a way as to increase the elastic compliance. It would appear that in the piezoelectric calculations, the charge Q is too low, so that the topology depends only on the elastic stiffness. However, the clearly different topologies shown in Fig. 7 for fixed polarization indicate that this is not the case: the charge $Q = 1$ μC – and therefore the electric energy – is large enough to influence the topology. It appears rather that the optimum topology obtained through the use of piezoelectric actuators is indeed very similar to the topology obtained through the (purely elastic) increase of stiffness by adding an extra layer.

6. Conclusions

The concept of topology optimization was successfully applied to find the optimal distribution of piezoelectric material in one or more layers of a multi-layer plate or shell structure to provide the minimum compliance when actuated. The design problem of layered piezoelectric plates and shells for minimum compliance was formulated and a new material model was proposed for piezoelectric materials based on the SIMP model. As a new feature, this model considers the change of piezoelectric polarization during the optimization, which is indispensable for obtaining an optimal design.

The developed optimization procedure was tested with an example, and the results confirm the proposed strategy and demonstrate the importance of including the polarization as an additional design variable. In the example, the algorithm determined a number of clearly distinct electrodes with different polarizations. The resulting design can be easily manufactured by using available technologies for bonding sensors and actuators on plate or shell surfaces.

7. Acknowledgments

The first author thanks the Deutsche Forschungsgemeinschaft (DFG – *German Research Council*), and all authors thank the University of São Paulo (Brazil) and the Fundação de Amparo à Pesquisa do Estado de São Paulo (FAPESP – *Research Support Foundation of São Paulo State*), Brazil for their support.

References

Agrawal, B. N. and Treanor, K. E. (1999). Shape control of a beam using piezoelectric actuators. *Smart Materials and Structures*, 8:729–740.

Bathe, K.-J. (1996). *Finite element procedures*. Prentice-Hall, Englewood Cliffs.

Bendsøe, M. P. (1989). Optimal shape design as a material distribution problem. *Structural Optimization*, 1:192–202.

Bendsøe, M. P. and Kikuchi, N. (1988). Generating optimal topologies in structural design using a homogenization method. *Computer Methods in Applied Mechanics and Engineering*, 71:197–224.

Bendsøe, M. P. and Sigmund, O. (2003). *Topology Optimization. Theory, Methods and Applications*. Springer-Verlag, Berlin.

Brei, D. and Moskalik, A. J. (1997). Deflection performance of a bi-directional distributed polymeric piezoelectric micromotor. *Journal of Microelectromechanical Systems*, 6(1):62–69.

Bucalem, M. L. and Bathe, K.-J. (1997). Finite element analysis of shell structures. *Archives of Computational Methods in Engineering*, 4(1):3–61.

Chattopadhyay, A., Seeley, C. E., and Jha, R. (1999). Aeroelastic tailoring using piezoelectric actuation and hybrid optimization. *Smart Material and Structures*, 8:83–91.

Díaz, A. R., Lipton, R., and Soto, C. A. (1995). A new formulation of the problem of optimum reinforcement of Reissner-Mindlin plates. *Computer Methods in Applied Mechanics and Engineering*, 123:121–139.

Gaul, L., Kögl, M., and Wagner, M. (2003). *Boundary Element Methods for Engineers and Scientists*. Springer-Verlag, Berlin.

Hanson, R. and Hiebert, K. (1981). *A Sparse Linear Programming Subprogram*. Sandia National Laboratories. Technical Report SAND81-0297.

Kögl, M. (2002). MITC plate elements for dynamic piezoelectric analyses. Research report, Department of Structures and Foundation Engineering, University of São Paulo.

Kögl, M. and Bucalem, M. (2002). Piezoelectric MITC plate elements. In *Proceedings of the Fifth World Congress on Computational Mechanics (WCCM V), July 7–12, 2002, Vienna, Austria,* `http://wccm.tuwien.ac.at`.

Kögl, M. and Bucalem, M. (2003). Locking-free piezoelectric MITC shell elements. In *Proceedings of the Second M.I.T. Conference on Computational Fluid and Solid Mechanics, M.I.T., Cambridge, USA*.

Kumar, A. V. and Gossard, D. C. (1996). Synthesis of optimal shape and topology of structures. *Transactions of the ASME*, 118:68–74.

Mukherjee, A. and Joshi, S. (2002). Piezoelectric sensor and actuator spatial design for shape control of piezolaminated plates. *AIAA Journal*, 40(6):1204–1210.

Saravanos, D. A. (1997a). Generalized finite element formulation for smart multilayered thermal piezoelectric composite plates. *Int. J. Solids Structures*, 34(26):3355–3371.

Saravanos, D. A. (1997b). Mixed laminate theory and finite element for smart piezoelectric composite shell structures. *AIAA Journal*, 35(8):1327–1333.

Silva, E. C. N. and Kikuchi, N. (1999). Design of piezoelectric transducers using topology optimization. *Smart Mater. Struct.*, 8:350–364.

Silva, E. C. N., Nishiwaki, S., and Kikuchi, N. (2000). Topology optimization design of flextensional actuators. *IEEE Transactions on Ultrasonics, Ferroelectrics and Frequency Control*, 47(3):657–671.

Suzuki, K. and Kikuchi, N. (1991). A homogenization method for shape and topology optimization. *Computer Methods in Applied Mechanics and Engineering*, 93:291–318.

Tzou, H. S. and Tseng, C. I. (1990). Distributed piezoelectric sensor/actuator design for dynamic measurement/control of distributed parameter systems: a piezoelectric finite element approach. *J. Sound Vibration*, 138(1):17–34.

Vanderplaatz, G. (1984). *Numerical Optimization Techniques for Engineering Design: with Applications*. McGraw-Hill, New York.